Accepted Manuscript

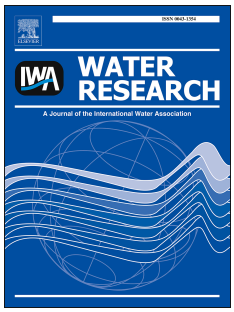

Iopromide exposure in *Typha latifolia* L.: Evaluation of uptake, translocation and different transformation mechanisms *in planta*

Hao Cui, Martin Hrabé de Angelis, Peter Schröder

PII: S0043-1354(17)30478-5

DOI: 10.1016/j.watres.2017.06.004

Reference: WR 12958

To appear in: *Water Research*

Received Date: 14 February 2017

Revised Date: 9 May 2017

Accepted Date: 3 June 2017

Please cite this article as: Cui, H., de Angelis, Martin.Hrabé., Schröder, P., Iopromide exposure in *Typha latifolia* L.: Evaluation of uptake, translocation and different transformation mechanisms *in planta*, *Water Research* (2017), doi: 10.1016/j.watres.2017.06.004.

Title: Iopromide exposure in *Typha latifolia* L.: Evaluation of uptake, translocation and different transformation mechanisms *in planta*.

Hao Cui[1], Martin Hrabé de Angelis[2], Peter Schröder[1]*

1. Research Unit Environmental Genomics, Helmholtz Zentrum München, German Research Center for Environmental Health, Ingolstaedter Landstr. 1, 85764 Neuherberg, Germany

2. Institute of Experimental Genetics, Helmholtz Zentrum München, German Research Center for Environmental Health, Ingolstaedter Landstr. 1, 85764 Neuherberg, Germany

*Author for correspondence

Mail address: peter.schroeder@helmholtz-muenchen.de

Tel: +49-89-3187-4056

Fax: +49-89-3187-3382

Abstract

Iopromide is frequently detected in water bodies due to its widespread use as an X- ray contrast agent in medicine. Due to its rapid clearance from the human body and its incomplete removal by wastewater treatment, an elevation of its concentration in the environment is observed that might lead to a serious impact on human and environmental health. Alternative or additional removal technologies may be more effective to remove iopromide from the effluents of wastewater treatment facilities, like phytoremediation with aquatic macrophytes. To test this, a hydroponic experiment was carried out to assess the fate of iopromide in *Typha latifolia*. The transformation products (TPs) in plant were investigated to predict the possible transformation mechanisms. The removal process followed first order kinetics with a linear regression R^2 value of 0.983. The iopromide concentration in roots and rhizomes reached a maximum value of 20.70±0.81 and 16.82±1.78 nmol·g^{-1} on the 7th day, respectively, thereafter decreased until the end of experiment. A different result was found in leaves, where iopromide concentration decreased over the whole experimental period. A total of eight transformation products were detected in *T. latifolia,* including 23 isomers. The relative content of aldehyde and ketone TPs decreased in roots and rhizomes while the relative content of carboxylic TPs increased. However, the relative content of aldehyde and ketone TPs only showed a slight decrease in leaves while the relative content of carboxylic TPs remained stable during the experimental period. In addition, a significantly increase of decarboxylated TPs was found in leaves, but not in roots and rhizomes. These results indicate that a difference of transformation mechanisms exists among plant tissues. The findings of this study are important to better understand the transformation mechanisms of iopromide in plants and to improve phytoremediation technologies for such kind of compounds.

TOC/Abstract Art

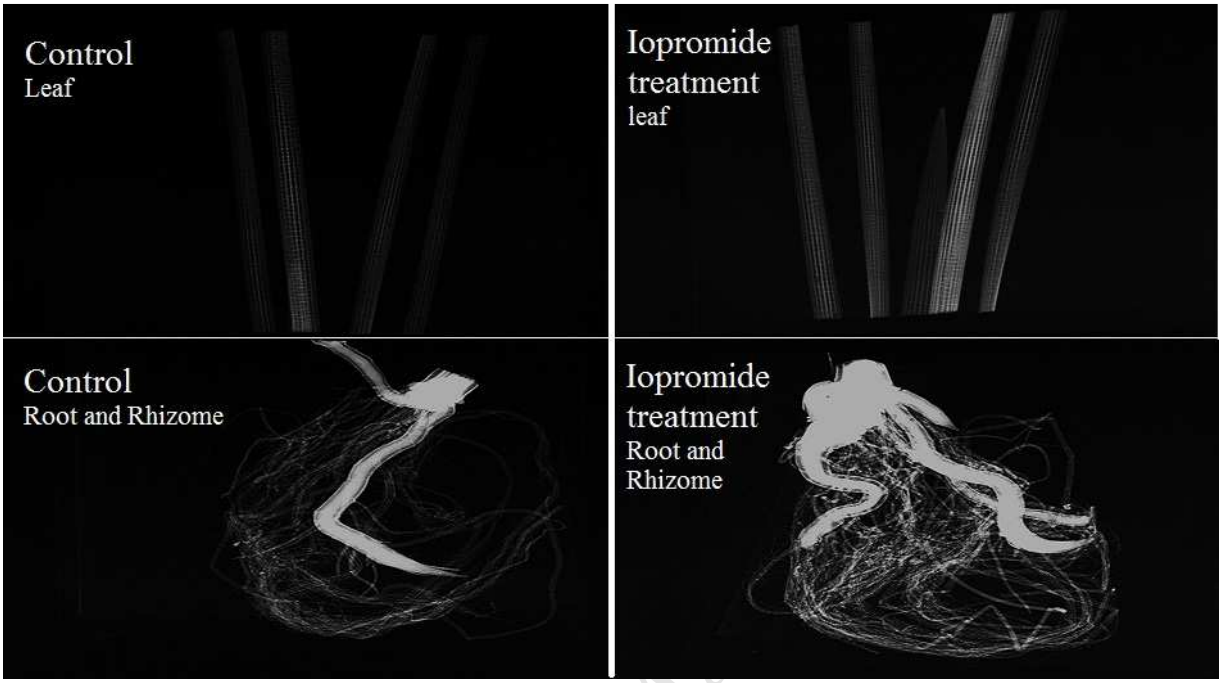

1. INTRODUCTION

Iodine containing X-ray contrast media are used to enhance the contrast of structures within the body in medical imaging. Especially the non-ionic iodine contrast media are widely used today as they are quickly spread and stable in the human body. Since increasingly higher amounts of such compounds are in use throughout Europe, it is not surprising that such compounds are frequently detected in wastewater effluents and surface waters (Mendoza et al., 2016; Zonja et al., 2015). Despite its beneficial properties, iopromide has been shown to induce oxidative stress and apoptosis in human neutrophils (Kayan et al., 2012). Iodine contrast media can form many transformation products (TPs) during wastewater and drinking water treatment processes, which might possess higher toxicity than the parent compounds (Duirk et al., 2011). Therefore, chronic exposure to these TPs may represent a non-negligible risk for aquatic organisms and human health.

Iopromide is one of the most frequently used X-ray contrast media. With high doses of usage (15g) and rapid excretion, it leaves the body almost unchanged (>95%) within a short time (Quinn et al.,1994; Schulz et al., 2008; Singh et al., 2014). Hence it is not surprising that this contrast agent has been detected in wastewater and in surface water at concentrations ranging from $ng \cdot L^{-1}$ to $\mu g \cdot L^{-1}$ (Kormos et al., 2011; Kovalova et al., 2012). And, importantly, the scientific concern is more on the formation of iodinated disinfection byproducts (DBPs). Previous studies have detected many toxic DBPs formed by chlorination of X-ray contrast media (Duirk et al., 2011; Wendel et al., 2014). Richardson et al. (2008) reported that iodinated DBPs have enhanced mammalian cell toxicity as compared to their brominated and chlorinated analogues. However, up to now, the generated DBPs cannot be effectively removed during sewage water treatment processes.

Phytoremediation is a plant-based approach to water remediation that takes advantage of low cost, simple operation and environmental friendliness (Zhang et al., 2014). An increasing number of studies found that aquatic plant-based systems have been highly efficient in the removal of emerging contaminants (Bartha et al., 2014; Yan et al., 2016; Zhang et al., 2013a; Zhang et al., 2016). In contrast to the traditional wastewater treatment process, phytoremediation can realize the removal of contaminants from the aqueous phase by plant uptake and subsequently bio-transform/accumulate these organics in the tissues. Hence, adding this technology could effectively avoid the secondary pollution by TPs and reduce environmental and human health risks. But so far, specific investigations of plant uptake and biological transformation are scarce (Imfeld et al., 2009).

The present study aimed at the uptake and translocation of iopromide using cattail (*Typha latifolia*) cultivated in hydroponic exposure. To highlight the transformation of iopromide in plants, the tissue distribution of iopromide and its TPs were assessed during different incubation times. Based on the results obtained in this study, the mechanism of plant-based transformation of iopromide has been further explored.

2. MATERIALS AND METHODS

Chemicals. Iopromide (98.6%) was purchased from Sigma (Germany). Solvents were LC-MS grade and obtained from Roth (Germany). All other chemicals were analytical grade. Ultrapure water was obtained from a Milli-Q water purification system.

Plant Materials. *Typha latifolia* plants were ordered from a local plant nursery (Jörg Petrowsky, Eschede, Germany) and carefully washed with tap water to remove adherent soil and debris. Plants were grown in perlite in 5L pots under greenhouse conditions with 12h of light/12h of darkness at 23/18°C and a humidity of 65%. Nutrients were provided in water by a modified Hoagland's nutrient solution. Plants uniform in size were selected for hydroponic experiment after acclimated to greenhouse conditions for two months. The composition of the nutrient solution was: 2.5 mmol·L^{-1} K^{+}, 2.0 mmol·L^{-1} Mg^{2+}, 2.0 mmol·L^{-1} Ca^{2+}, 2.0 mmol·L^{-1} SO_4^{2-} , 6.0 mmol·L^{-1} NO_3^{-}, 0.5 mmol·L^{-1} $H_2PO_4^{-}$,50 μmol·L^{-1} Fe^{2+}, 50 μmol·L^{-1} BO_3^{3-}, 1 μmol·L^{-1} Mn^{2+}, 0.5 μmol·L^{-1} Cu^{2+}, 0.5 μmol·L^{-1} Zn^{2+}, 0.1 μmol·L^{-1} $MoO_4^{2-}$and the pH was adjusted to 6.0.

Hydroponic Experiment Setup. Plant rhizomes were rinsed with distilled water and then transferred to 2.5 L plastic pots. The pots were covered with plastic package inside to prevent the potential adsorption of iopromide on the pot surface. Each pot contained 1 L nutrient solution and 1L perlite to fix the plant. The nutrient solution was spiked with iopromide to reach a final initial concentration of 20 μmol·L^{-1}. Pots with equal concentration of iopromide but without plants were used as controls. The loss of nutrient solution was countered by daily weighing and filling the pots to the starting volumes. Three replicates of controls and each exposure period studied were set up, i.e., 1, 3, 7, 14 and 28 days. For each exposure period, root, leaf, rhizome and nutrient solutions were collected, rinsed with distilled water and wiped dry with lab tissue, then frozen and stored at -80°C.

X-Ray of exposed plant tissues. Plant rhizomes and roots were thoroughly washed and blotted dry with filter paper, leaves were excised, cut to uniform length and all plant parts were quickly placed in Teflon bags (10x10 cm) and sealed. X-rays were taken with a Faxitron MX-20 DC-12 system (Faxitron Bioptics, LLC, 3440 E Britannia Dr, Suite 150, Tucson, Arizona 85706 USA)

under automated setting. Images were taken by the implemented camera system and stored as digital files.

Analysis of Iopromide and its TPs by Liquid Chromatography Tandem Mass Spectrometry (LC-MS/MS). The determination of iopromide in water and plant followed our previous work. Briefly, 0.5 g fresh plant material was ground under liquid nitrogen and then extracted with 4.5 mL extraction solution (water with 0.1% formic acid). The mixture was homogenized, ultrasonicated, centrifuged and then the supernatant was filtrated through a 0.45 μm Nylon filter. The filtrates were transferred to a solid phase extraction (SPE) column (Oasis HLB, Waters, Germany), percolated, washed and eluted. When the extraction processes was calibrated by the use of blank plant tissue spiked with iopromide, the recovery was > 90%. Subsequently, the analytes were injected into the LC-MS/MS system.

The HPLC system (Varian ProStar 210, Darmstadt, Germany) was coupled to an ion trap mass spectrometer (Varian 500-MS, Darmstadt, Germany) via an electrospray ionization source. Separation was achieved on a Synergi Polar-RP 80a column (150 mm × 2 mm, 4μm, Bischoff, Germany) at a flow rate of 0.3 $mL \cdot min^{-1}$. For the determination of iopromide, the precursor ion *m/z* 791.8 $(M+H)^+$ yielding fragment ions *m/z* 773.8 and *m/z* 572.9 was used for quantification and confirmation.

3. RESULTS AND DISCUSSION

Removal of Iopromide from the Medium. Iopromide was removed from the nutrient solution by *T. latifolia*, and the removal efficiency increased with exposure time. The maximum removal

efficiency was 86.6±2.3% after 28 days (Figure 1). The removal process satisfied the first-order kinetic equation as well as the decay rate constant of 0.0783 day^{-1} with a linear regression R^2 value of 0.983 (Supplementary information, Figure S1). No significant variation of iopromide concentration in the medium was found in controls during the whole experimental period.

Previous studies had shown that pharmaceuticals can be removed by plants. Dordio et al. (2011) reported carbamazepine removal by *Typha spp.* with removal efficiencies ranging between 56%~82% for different initial concentrations. Reinhold et al. (2010) indicated that in an active duckweed reactor which consisted predominantly of *L. minor* or *L. punctata*, ibuprofen concentrations decreased linearly to 47.5% depletion in 9 d. Zhang et al. (2013a) found the removal processes of five different pharmaceuticals by *Scirpus validus* were also following first-order, and the decay rate constants in a range of 0.023~0.403 day^{-1}. Adsorption and photodegradation of iopromide seemed to play only a minor role during the experimental period since no significant variation was found in controls. Therefore, the elimination of iopromide is hypothezised to be highly dependent on the uptake by plants.

Uptake and Translocation of Iopromide by *T. latifolia*. Iopromide was detected in extracts of all plant tissues, including roots, rhizomes and leaves during the whole exposure period. When plant parts were x-rayed with standard x-ray equipment, lignified or suberized tissues appeared greyish/white, with a higher intensity in freshly developed rhizomes, and cell walls. Since iopromide functions as a contrast agent by opacifying vessels in the path of flow of the contrast agent, radiographic visualization of the internal structures that had been reached by the compound, and hence compound localization became possible. Plants treated with iopromide showed distinctly higher whitening in roots, rhizomes, and stronger display of the veins of the leaves (Figure S2). In roots and rhizomes, iopromide concentrations increased with exposure

time up to day 3, remained stable until day 7 and decreased thereafter (Figure 2). The maximum iopromide concentration in roots was found to be 20.70±0.81 nmol·g^{-1} (fresh weight) while in rhizomes 16.82±1.78 nmol·g^{-1} (fresh weight) accumulated after 7 days of exposure. Iopromide concentration in leaves decreased constantly with exposure time (Figure 2). The iopromide concentration in leaves was 2.00±0.22 nmol·g^{-1} (fresh weight) at day 1, and gradually decreased to 0.34±0.05 nmol·g^{-1} (fresh weight) at day 28. Compared to roots and rhizomes, iopromide concentration was relatively low in leaves, as had also been visible in the x-ray pictures. Table S1 shows the bioaccumulation factors for all plant tissues, ranging from 0.02 to 1.04.

Plant uptake of foreign compounds consists of both, the apoplastic and symplastic pathway. The free apoplastic flow is finally forced to move into the symplast pathways as the root endodermis contains the casparian strip, blocking the uptake of undesirable compounds (Sperry et al., 2002). Thus, the transmembrane transport of contaminants plays a decisive role in the uptake processes. Organic contaminants tend to move into plant roots driven by passive diffusion (Pilon-Smits, 2005). Therefore, uptake of xenobiotics seems to be dependent on their physico-chemical properties, especially their Log P, but also their apparent molecular diameter, and molecular weight. Not surprisingly, our results demonstrate higher iopromide concentration in roots than in leaves. This result is consistent with that of Herklotz and coworkers who find that Salbutamol (Molecular weight = 239.3Da), a smaller more hydrophobic molecule, also exhibits strong accumulation in cabbage roots (Herklotz et al., 2010). Uptake of iopromide into the roots was relatively fast up to day 3 (Figure 2). This result is in line with previous studies showing uptake of xenobiotics by plants within a short time (Li et al., 2005; Zhang et al., 2013b). Similar high initial uptake rates were also reported for other pharmaceuticals in previous studies (Bartha et al., 2014; Herklotz et al., 2010; Zhang et al., 2013b). Generally, organic compounds with an

optimum hydrophobicity (logP = 0.5~3) seem to be translocated in plant tissues via the symplastic pathway. However, recent studies indicate that hydrophilic chemicals can also have great potential to be taken up and translocated by plants (Yamazaki et al. 2015).

Iopromide was detected early in leaves, and its steadily decreasing concentration suggests that it is successively transformed in leaf tissues. In theory, there should be an equilibrium between iopromide intake and iopromide dissipation. In roots and rhizomes, the iopromide intake mainly represents uptake while the iopromide dissipation is composed of translocation to leaves and transformation. In leaves, the iopromide intake mainly consists of translocation from roots and the iopromide dissipation includes transformation. At the onset of the experiments, the intake rate was higher than the disappearance rate in roots and rhizomes. Since the iopromide concentration decreased in medium with time, the intake rate decreased while the disappearance increased. As a result, iopromide concentrations in roots and rhizomes increased to a high level remaining constant for some time and decreased thereafter due to accelerated metabolism.

Different transformation mechanisms of Iopromide in *T. latifolia*. A total of 8 TPs including 23 isomers were detected when iopromide was metabolized by *T. latifolia*. These TPs were not detected in the nutrient solution, which lets us propose that the entire transformation occurs in planta. The structures of these TPs were identified by LC-MS/MS, and to unravel the transformation mechanisms, these TPs were analyzed at five different time points during incubation. Iopromide transformation by *T. latifolia* could be divided into four reactions: I) the hydroxyl groups being oxidized to aldehyde or ketone groups, II) aldehyde groups being oxidized to carboxyl groups, III) decarboxylation, IV) deiodination.

193 The temporal progression of TPs formation in roots is shown in Figure 3, where the indicated
194 relative content is a ratio of one TP amount to the total TPs amount in the plant tissue. There is a
195 trend of decrease in the content of TP789A and B with the extension of inoculation time. The
196 sum of the relative content of TP789A and B were 48.3% at day 1, then continually decreased to
197 7.0% at day 28. This indicates that TP789A and B are probably the main precursor compounds
198 for most of the other TPs. Thus, the oxidation of a hydroxyl group into aldehyde or ketone
199 groups seems to be the first step of iopromide transformation in *T. latifolia* roots. TP787 A, B
200 and C were formed from TP789 by further oxidation of the hydroxyl group. The relative content
201 of TP787A increased until day 14 then remained stable similar to TP787B for which also no
202 significant variation was observed. The relative content of TP787C increased in the first 14 days
203 and thereafter decreased.

204 Reaction I is known and approved to be catalyzed by alcohol dehydrogenases, which have been
205 shown to commonly exist in bacteria and higher plants (Kroutil et al., 2004). Nicotinamide
206 adenine dinucleotide (NAD^+) is the acceptor during the enzymatic oxidative dehydrogenation
207 process. Some studies indicate that peroxidase and monooxygenase can also be responsible for
208 this type of reaction in plants (Kroutil et al., 2004; Geigert et al., 1983). Our results show an
209 increasing relative content of TP787A than TP787B over time. This is probably due to the
210 difference between the structure of side chain A and side chain B. Several NADH-dependent
211 enzymes (i.e. methylglyoxal reductase) may contribute to the transformation from TP789 (A and
212 B) and TP787 (A and B).

213 The relative content of TP805A in roots and rhizomes increased in the first two weeks followed
214 by a plateau. In leaves, the relative content of TP805A decreased with time. For TP805B in roots

and rhizomes, the relative content decreased until day 7, then increased with time, while no significant trend was found in leaves (Figure 4).

Generally, carboxylic TPs were formed from aldehydic TPs. Aldehyde dehydrogenases, which are probably responsible for this chemical reaction, have been found in different organisms (Sophos et al., 2001; Muzio et al., 2012). Several aldehyde dehydrogenase genes have been identified in plant species (Sunkar et al., 2003; Liu and Schnable, 2002). It has been shown that aldehyde dehydrogenases can oxidize both aliphatic aldehydes and aromatic aldehydes in maize.

The relative content of TP803A in roots was stable in the first two weeks. After that, an increase followed, while in rhizomes a continuous increasing trend was observed. For TP803B, a stable period in the first week followed by an increase was observed in both roots and rhizomes. In leaves, the relative content of both TP803A and B remained stable in the first week, and thereafter increased until the end of incubation. The total relative content of both TP803A and B presents a steadily increasing trend in all plant tissues, except on day 7 when it decreased slightly in leaves (Figure 4).

The relative content of TP819 showed an increasing trend in roots, while on the contrary, a decreasing trend in leaves was observed. The relative content increased in the first two weeks followed a slight decrease in rhizomes. The relative content of both TP817 A and B remained stable in the first week in all plant tissues then started increasing in roots and rhizomes but decreasing in leaves. The relative content of TP815 reached a maximum of 0.69% at day 7 in roots, while 1.70% at day 3 in rhizomes. An increasing trend of the relative content of TP815 with time was found in leaves (Figure 4).

The precise mechanism of the formation of carboxylic TPs in the investigated species is not yet known. Mechanisms involving the oxidation of lactic acid are possible, and such a reaction may be catalyzed by lactate dehydrogenase in plants. Glycolate oxidase catalyzes the oxidation of glycolic acid to glyoxylate in the peroxisomes during photorespiration (Taler et al., 2004). The glycolate oxidase is mainly expressed in green leaves, and may be responsible for the formation of TP815 (Clagett et al., 1949). This could be an explanation for the increasing trend of the TP815 relative content in leaves with time. Because TP819 and TP817 could be further oxidized, the product accumulating in leaves might be TP815 which is probably also the end product of the carboxylic TPs type. Carboxylic TPs were the major kind of iopromide TPs in *T. latifolia* (Figure 4). Aldehydes are known to be toxic to the plants. Therefore, an oxidation of aldehydes TPs to carboxylic TPs in plant tissues would be expected. This transformation is in accordance with the aldehyde detoxification mechanisms in plants.

The relative content of TP787D decreased in the first two weeks in roots and rhizomes, thereafter it increased until the end of incubation time. On the contrary, the relative content of TP787D increased in the first two weeks in leaves before its concentration reached a plateau (Figure 5). Based on molecular structure of TP787D, we suggest TP787D is probably formed from decarboxylation of TP815. Many different enzymes can catalyze this reaction, such as α-keto acid-dependent dioxygenases and branched-chain α-keto acid dehydrogenases (Damuni et al., 1984; Hegg et al., 1999).

The relative content of TP665 reached a maximum of 4.50% at day 14 in roots, thereafter decreased to 1.33% at the end of incubation. In leaves, the relative content of TP665 showed a slight increasing trend until day 14 and a stronger accumulation until the end of incubation, while a broadly stable trend has been found in rhizomes (Figure 5).

Dehalogenation has been found in plants during the degradation of halogenated aromatic contaminants. Wang et al. (2012) reported that debromination was catalyzed in maize after the exposure to polybrominated diphenyl ethers. Recently, Sun et al. (2013) also found debromination from brominated diphenyl ether-47 to brominated diphenyl ether-28 in young pumpkin plants. However, further debromination products were not detected in those studies. Schulz and coworkers (2008) and Singh and coworkers (2015) described deiodination of iopromide TPs by microbial activity and advanced oxidation processes, respectively, considering different possible structures since it remained unclear which I-atom had been removed. This is similar to our results which only found deiodination from iopromide to TP665, but no further deiodinated TPs.

Many reductive dehalogenases have been found in bacteria which are responsible for catalyzing dehalogenation of aromatic ring systems (Anandarajah et al., 2000; Payne et al., 2015). However, little information has been found in plants. Among other enzymes, glutathione S-transferase can catalyze the reductive degradation of xenobiotics in plants. However, typical related intermediates of a substitution reaction (i.e. glutathione conjugates) were not detected in this study. We suggest that reductive dehalogenation might occur while the conjugate formation is probably inhibited due to steric effects of the side chains. Recently van Aken and coworkers (2010) summarized several plant enzyme catalyzed dehalogenation processes employing unexpected enzymatic agents. Further studies are required to scrutinize this important degradation step.

4. CONCLUSION

The results of this study clearly show that iopromide can be taken up by *T. latifolia* and the removal efficiency increases with exposure time. Therefore, phytoremediation can be an effective way to eliminate such polar pharmaceuticals from water. The maximum iopromide concentration in roots and rhizomes was found at 3rd day, indicating that iopromide can be rapidly degraded in plants. Thus it is essential to clearly understand the transformation mechanisms of such pollutants in plants. Further research is needed to evaluate the toxicity of the most prominent iopromide TPs.

Acknowledgments

We thank Daniel Feeser for the help in X-ray analysis. This research was stimulated by COST Action ES 1202: Conceiving Wastewater Treatment in 2020-Energetic, environmental and economic challenges (Water-2020).

5. REFERENCES

Anandarajah, K., Kiefer, P.M.Jr., Donohoe, B.S., Copley, S.D. 2000. Recruitment of a double bond isomerase to serve as a reductive dehalogenase during biodegradation of pentachlorophenol. Biochemistry. 39 (18), 5303-5311.

Bartha, B., Huber, C., Schröder, P. 2014. Uptake and metabolism of diclofenac in *Typha latifolia* – How plants cope with human pharmaceutical pollution. Plant. Sci. 227, 12-20.

Clagett, C.O., Tolbert, N.E., Burris, R.H. 1949. Oxidation of alpha-hydroxy acids by enzymes from plants. J. Biol. Chem. 17 (2), 977-987.

Damuni, Z., Merryfield, M.L., Humphreys, J.S., Reed, L.J. 1984. Purification and properties of branched-chain alpha-keto acid dehydrogenase phosphatase from bovine kidney. Proc. Natl. Acad. Sci. USA. 81 (14), 4335-4338.

Dordio, A.V., Belo, M., Martins Teixeira, D., Palace Carvalho, A.J., Dias, C.M.B., Picó, Y., Pinto, A.P. 2011. Evaluation of carbamazepine uptake and metabolization by *Typha spp*., a plant with potential use in phytotreatment. Bioresource. Technol. 102 (17), 7827-7834.

Duirk, S.E., Lindell, C., Cornelison, C.C., Kormos, J., Ternes, T.A., Attene-Ramos, M., Osiol, J., Wagner, E.D., Plewa, M.J., Richardson, S.D. 2011. Formation of toxic iodinated disinfection by-products from compounds used in medical imaging. Environ. Sci. Technol. 45 (16), 6845-6854.

Geigert, J., Dalietos, D.J., Neidleman, S.L., Lee, T.D., Wadsworth, J. 1983. Peroxide oxidation of primary alcohols to aldehydes by chloroperoxidase catalysis. Biochem. Bioph. Res. Co. 114 (3), 1104-1108.

311 Hegg, E.L., Whiting, A.K., Saari, R.E., McCracken, J., Hausinger, R.P., Que, L.Jr. 1999.
312 Herbicide-degrading alpha-keto acid-dependent enzyme TfdA: metal coordination environment
313 and mechanistic insights. Biochemistry. 38 (50), 16714-16726.

314 Herklotz, P.A., Gurung, P., Vanden Heuvel, B., Kinney, C.A. 2010. Uptake of human
315 pharmaceuticals by plants grown under hydroponic conditions. Chemosphere. 78 (11),
316 1416-1421.

317 Imfeld, G., Braeckevelt, M., Kuschk, M.P., Richnow, H.H. 2009. Monitoring and assessing
318 processes of organic chemicals removal in constructed wetlands. Chemosphere. 74 (3), 349-362.

319 Kayan, M., Nazıroğlu , M., Övey, İ, Aykur, M., Uğuz, A., Yürekli, V. 2012. Non-Ionic contrast
320 media induces oxidative stress and apoptosis through Ca^{2+} influx in human neutrophils. J.
321 Membrane. Biol. 245 (12), 833-840.

322 Kormos, J.L., Schulz, M., Ternes, T.A. 2011. Occurrence of Iodinated X-ray Contrast Media and
323 Their Biotransformation Products in the Urban Water Cycle. Environ. Sci. Technol. 45 (20),
324 8723-8732.

325 Kovalova, L., Siegrist, H., Singer, H., Wittmer, A., McArdell, C.S. 2012. Hospital wastewater
326 treatment by membrane bioreactor: performance and efficiency for organic micropollutant
327 elimination. Environ. Sci. Technol. 46 (3), 1536-1545.

328 Kroutil, W., Mang, H., Edegger, K., Fabe, K. 2004. Biocatalytic oxidation of primary and
329 secondary alcohols. Adv. Synth. Catal. 346 (2-3), 125-142.

330 Li, H., Sheng, G., Chiou, C.T., Xu, O. 2005. Relation of organic contaminant equilibrium
331 sorption and kinetic uptake in plants. Environ. Sci. Technol. 39 (13), 4864-4870.

Liu, F., Schnable, P.S. 2002. Functional specialization of maize mitochondrial aldehyde dehydrogenases. Plant. Physiol. 130 (4), 165-1674.

Mendoza, A., Zonja, B., Mastroianni, N., Negreira, N., López de Alda, M., Pérez, S., Barceló, D., Gil, A., Valcárcel, Y. 2016. Drugs of abuse, cytostatic drugs and iodinated contrast media in tap water from the Madrid region (central Spain): A case study to analyse their occurrence and human health risk characterization. Environ. Int. 86, 107-118.

Muzio, G., Maggiora, M., Paiuzzi, E., Oraldi, M., Canuto, R.A. 2012. Aldehyde dehydrogenases and cell proliferation. Free. Radical. Bio. Med. 52 (4), 735-746.

Payne, K.A., Quezada, C.P., Fisher, K., Dunstan, M.S., Collins, F.A., Sjuts, H., Levy, C., Hay, S., Rigby, S.E., Leys, D. 2015. Reductive dehalogenase structure suggests a mechanism for B12-dependent dehalogenation. Nature. 517 (7535), 513-516.

Pilon-Smits, E. 2005. Phytoremediation. Annu. Rev. Plant. Biol. 56, 15-39.

Quinn, A.D., O'Hare, N.J., Wallis, F.J., Wilson, G.F. 1994. Gd-DTPA: an alternative contrast medium for CT. J. Comput. Assist. Tomogr. 18 (4), 634-636.

Reinhold, D., Vishwanathan, S., Park, J.J., Oh, D., Michael Saunders, F. 2010. Assessment of plant-driven removal of emerging organic pollutants by duckweed. Chemosphere. 80 (7), 687-692.

Richardson, S.D., Fasano, F., Ellington, J.J., Crumley, F.G., Buettner, K.M., Evans, J.J., Blount, B.C., Silva, L.K., Waite, T.J., Luther, G.W., McKague, A.B., Miltner, R.J., Wagner, E.D., Plewa, M.J. 2008. Occurrence and mammalian cell toxicity of iodinated disinfection byproducts in drinking water. Environ. Sci. Technol. 42 (22), 8330-8338.

353 Sperry, J.S., Stiller, V., Hacke, U.G. Soil Water uptake and water transport through root systems,
354 in: Waisel, Y., Eshel, A., Kafkafi, U., (Eds.), Plant Roots-The Hidden Half, Third Edition,
355 Marcel Dekker Inc., New York, 2002, pp. 1008-1040.

356 Schulz, M., Löffler, D., Wagner, M., Ternes, T.A. 2008. Transformation of the X-ray contrast
357 medium Iopromide in soil and biological wastewater treatment. Environ. Sci. Technol. 42 (19),
358 7207-7217.

359 Singh, R.R., Lester, Y., Linden, K.G., Love, N.G., Atilla-Gokcumen, G.E., Aga, D.S. 2014.
360 Application of metabolite profiling tools and time-of-flight mass spectrometry in the
361 identification of transformation products of iopromide and iopamidol during advanced oxidation.
362 Environ. Sci. Technol. 49 (5), 2983-2990.

363 Sophos, N.A., Pappa, A., Ziegler, T.L., Vasiliou, V. 2001. Aldehyde dehydrogenase gene
364 superfamily: the 2000 update. Chem. Biol. Interact. 130-132 (1-3), 323-337.

365 Sun, J.T., Liu, J.Y., Yu, M., Wang, C., Sun, Y.Z., Zhang, A.G., Wang, T., Lei, Z., Jiang, G.B.
366 2013. In vivo metabolism of 2,2 ',4,4 '-tetrabromodiphenyl ether (BDE-47) in young whole
367 pumpkin plant. Environ. Sci. Technol. 47 (8), 3701-3707.

368 Sunkar, R., Bartels, D., Kirch, H.H. 2003. Overexpression of a stress-inducible aldehyde
369 dehydrogenase gene from *Arabidopsis thaliana* in transgenic plants improves stress tolerance.
370 Plant. J. 35 (4), 452-464.

371 Taler, D., Galperin, M., Benjamin, I., Cohen, Y., Kenigsbuch, D. 2004. Plant eR genes that
372 encode photorespiratory enzymes confer resistance against disease. Plant. Cell. 16 (1), 172-184.

373 Van Aken, B., Correa, P.A., and Schnoor, J.L. (2010) Phytoremediation of Polychlorinated
374 Biphenyls: New Trends and Promises. Environ Sci Technol. 2010 April 15; 44(8): 2767–2776.

375 Wang, S., Zhang, S., Huang, H., Lu, A., Ping, H. 2012. Debrominated, hydroxylated and
376 methoxylated metabolism in maize (*Zea mays* L.) exposed to lesser polybrominated diphenyl
377 ethers (PBDEs). Chemosphere. 89 (11), 1295-1301.

378 Wendel, F.M., Lutke Eversloh, C., Machek, E.J., Duirk, S.E., Plewa, M.J., Richardson, S. D.,
379 Ternes, T.A. 2014. Transformation of iopamidol during chlorination. Environ. Sci. Technol. 48
380 (21), 12689-12697.

381 Yamazaki, K., Tsuruta, H. and Inui, H. (2015) Different uptake pathways between hydrophilic
382 and hydrophobic compounds in lateral roots of *Cucurbita pepo*. Journal of Pesticide Science
383 40(3), 99–105.

384 Yan, Q., Feng, G., Gao, X., Sun, C., Guo, J.S., Zhu, Z. 2016. Removal of pharmaceutically
385 active compounds (PhACs) and toxicological response of *Cyperus alternifolius* exposed to
386 PhACs in microcosm constructed wetlands. J. Hazard. Mater. 301, 566-575.

387 Zhang, D.Q., Gersberg, R.M., Hua, T., Zhu, J., Goyal, M.K., Ng, W.J., Tan, S.K. 2013a. Fate of
388 pharmaceutical compounds in hydroponic mesocosms planted with *Scirpus validus*. Environ.
389 Pollut. 181, 98-106.

390 Zhang, D.Q., Gersberg, R.M., Hua, T., Zhu, J., Ng, W.J., Tan, S.K. 2013b. Assessment of
391 plant-driven uptake and translocation of clofibric acid by *Scirpus validus*. Environ. Sci. Pollut. R.
392 20 (7), 4612-4620.

393 Zhang, D.Q., Gersberg, R.M., Ng, W.J., Tan, S.K. 2014. Removal of pharmaceuticals and
394 personal care products in aquatic plant-based systems: a review. Environ. Pollut. 184, 620-639.

395 Zhang, Y., Lv, T., Carvalho, P.N., Arias, C.A., Chen, Z., Brix, H. 2016. Removal of the
396 pharmaceuticals ibuprofen and iohexol by four wetland plant species in hydroponic culture: plant
397 uptake and microbial degradation. Environ. Sci. Pollut. R. 23 (3), 2890-2898.

398 Zonja, B., Delgado, A., Perez, S., Barcelo, D. 2015. LC-HRMS suspect screening for
399 detection-based prioritization of iodinated contrast media photodegradates in surface waters.
400 Environ. Sci. Technol. 49 (6), 3464-3472.

401

402 Legends to Tables and Figures

403 Table 1 Identification of iopromide and its transformation products in *T.latifolia.*

404

405 Figure 1. The removal efficiencies of iopromide by *T. latifolia* at different exposure time. Plotted
406 values are means ± SD of three replicates.

407 Figure 2. Concentrations of iopromide in different tissues of exposed *T. latifolia*. Plotted values
408 are means ± SD of three replicates.

409 Figure 3. Relative peak area trends of aldehyde and ketone transformation products identified in
410 *T. latifolia* during the experimental periods. Plotted values are means ± SD of three replicates.

411 Figure 4. Relative peak area trends of carboxylic transformation products identified in *T. latifolia*
412 during the experimental periods. Plotted values are means ± SD of three replicates.

413 Figure 5. Relative peak area trends of decarboxylated and deiodinated transformation products
414 identified in *T. latifolia* during the experimental periods. Plotted values are means ± SD of three
415 replicates.

Table 1

Compound	Molecular structure	[M-H]+ (m/z)	Molecular formula	Fragment ions (m/z)
Iopromide	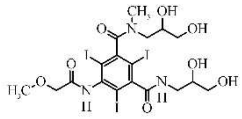	791.8	$C_{18}H_{25}O_8N_3I_3$	773.8, 572.9, 558.9
TP789A1-2	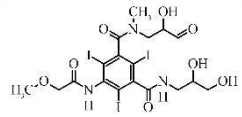	789.8	$C_{18}H_{23}O_8N_3I_3$	698.9, 686.8, 559.1
TP789B1-2	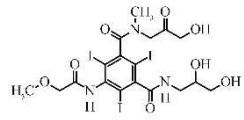	789.8	$C_{18}H_{23}O_8N_3I_3$	701.0, 699.9, 572.9
TP787A	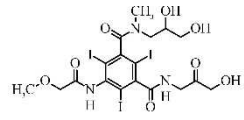	787.8	$C_{18}H_{21}O_8N_3I_3$	718.1, 686.9, 559.2
TP787B	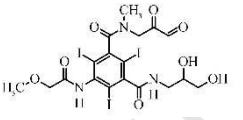	787.8	$C_{18}H_{21}O_8N_3I_3$	701.3, 700.0, 572.9
TP787C	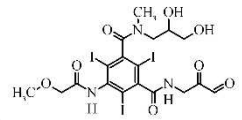	787.8	$C_{18}H_{21}O_8N_3I_3$	716.0, 698.9, 571.2

	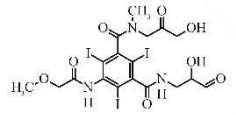			
	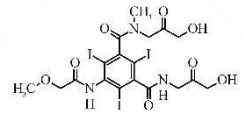			
TP805A	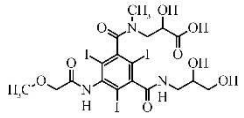	805.8	$C_{18}H_{23}O_9N_3I_3$	714.9, 587.2, 559.1
TP805B	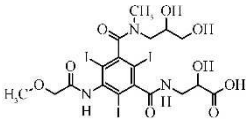	805.8	$C_{18}H_{23}O_9N_3I_3$	760.2, 700.7, 573.1
TP803A1-2	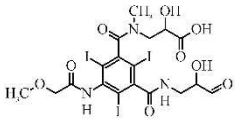	803.8	$C_{18}H_{21}O_9N_3I_3$	715.0, 684.9, 557.3
TP803B1-2	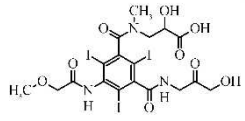	803.8	$C_{18}H_{23}O_9N_3I_3$	700.8, 698.9, 571.2
TP819	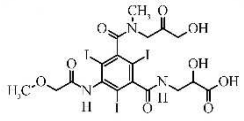	819.8	$C_{18}H_{21}O_{10}N_3I_3$	715.1, 700.8, 587.2
TP817A	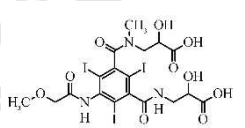	817.8	$C_{18}H_{21}O_{10}N_3I_3$	713.0, 700.9, 573.1

TP817B	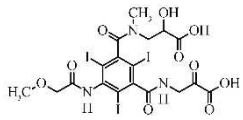	817.8	$C_{18}H_{21}O_{10}N_3I_3$	714.9, 699.0, 587.1
TP815	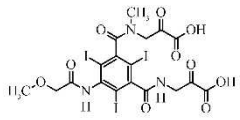	815.8	$C_{18}H_{17}O_{10}N_3I_3$	712.9, 670.0, 585.0
TP787D1	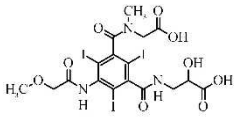	787.8	$C_{17}H_{17}O_9N_3I_3$	712.9, 671.0, 542.8
TP787D2	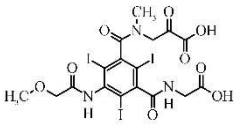	787.8	$C_{17}H_{17}O_9N_3I_3$	699.0, 684.8, 557.0
TP665	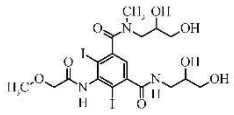	665.8	$C_{18}H_{26}O_8N_3I_2$	575.0, 561.0, 520.0

Figure 1

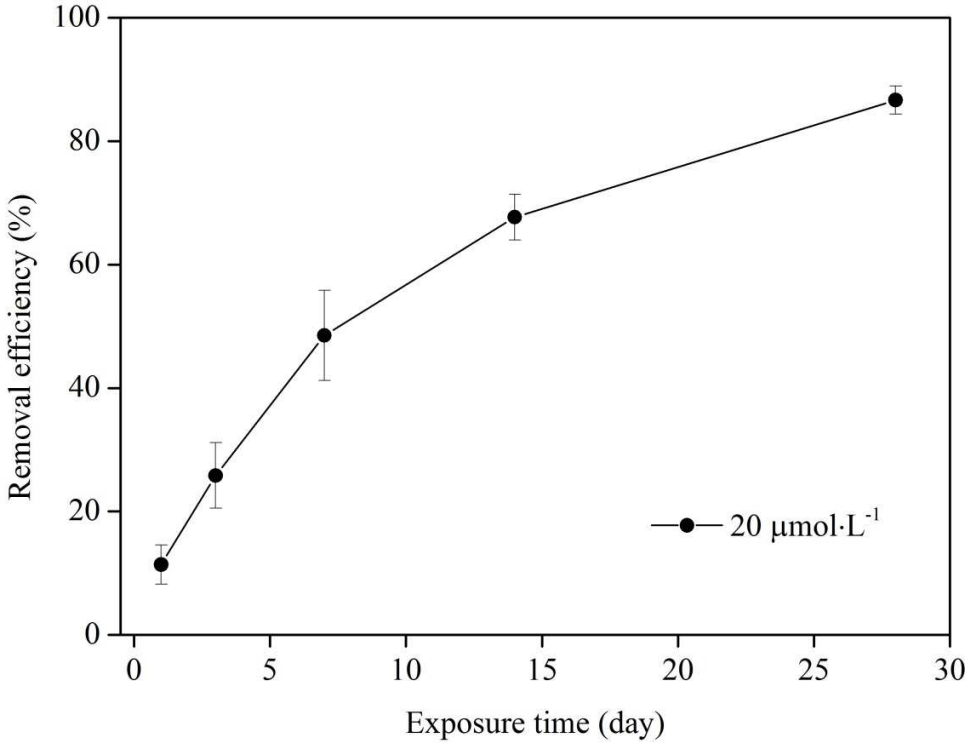

Figure 2

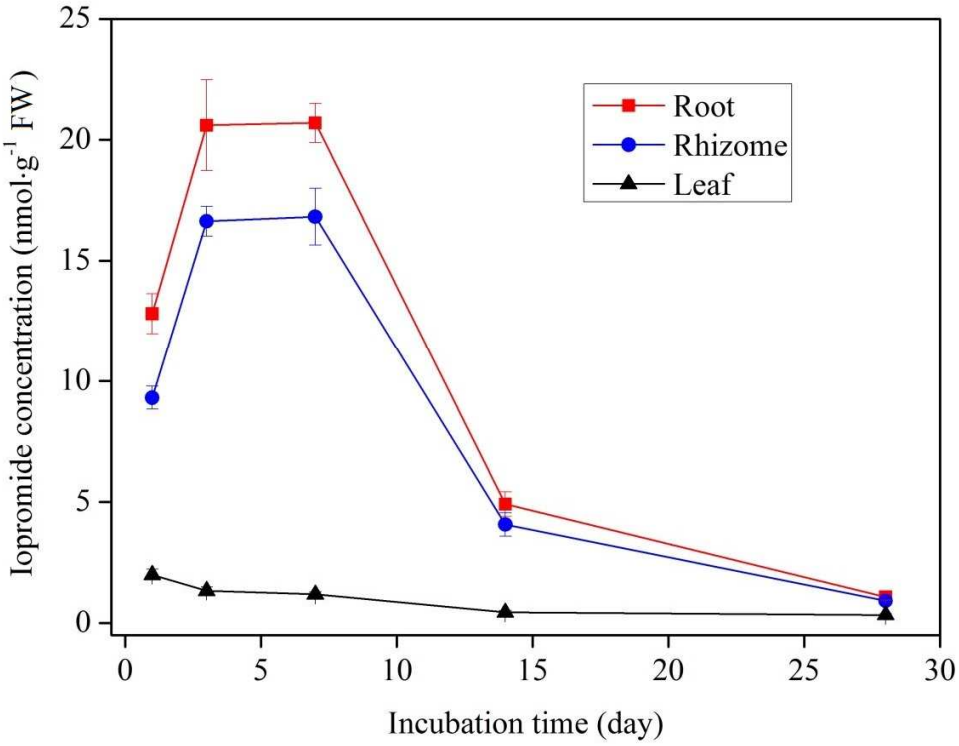

Figure 3

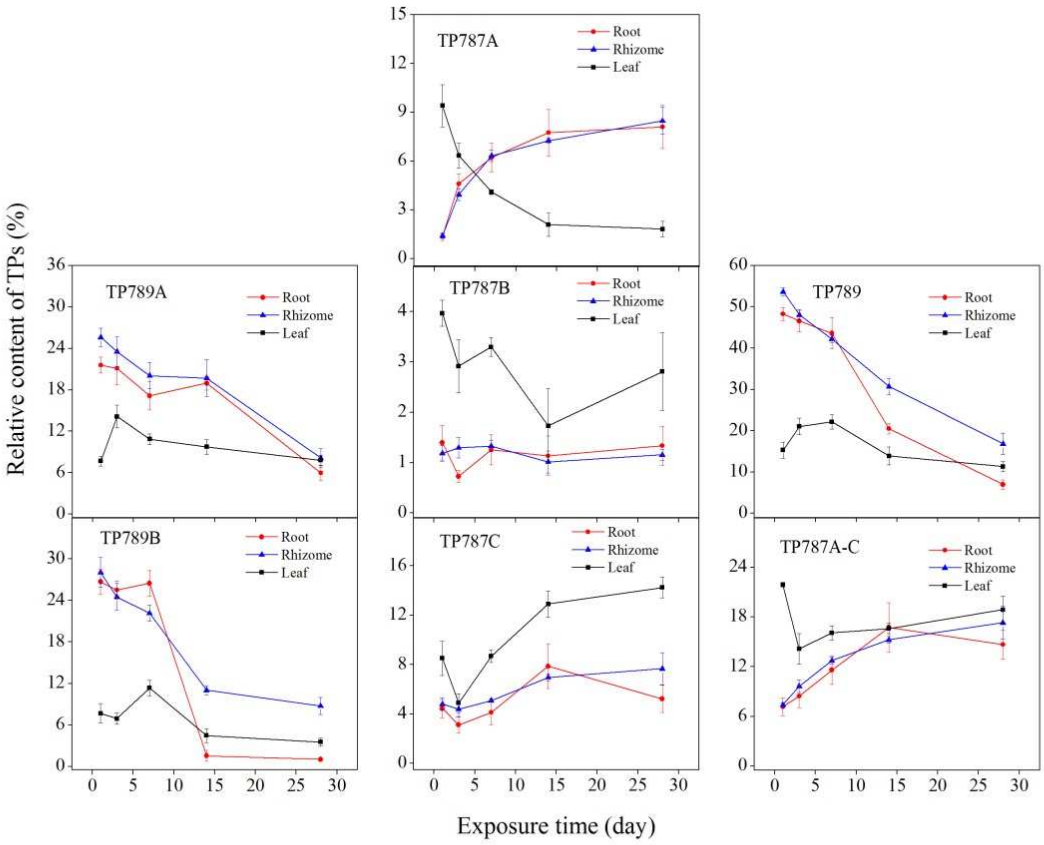

Figure 4

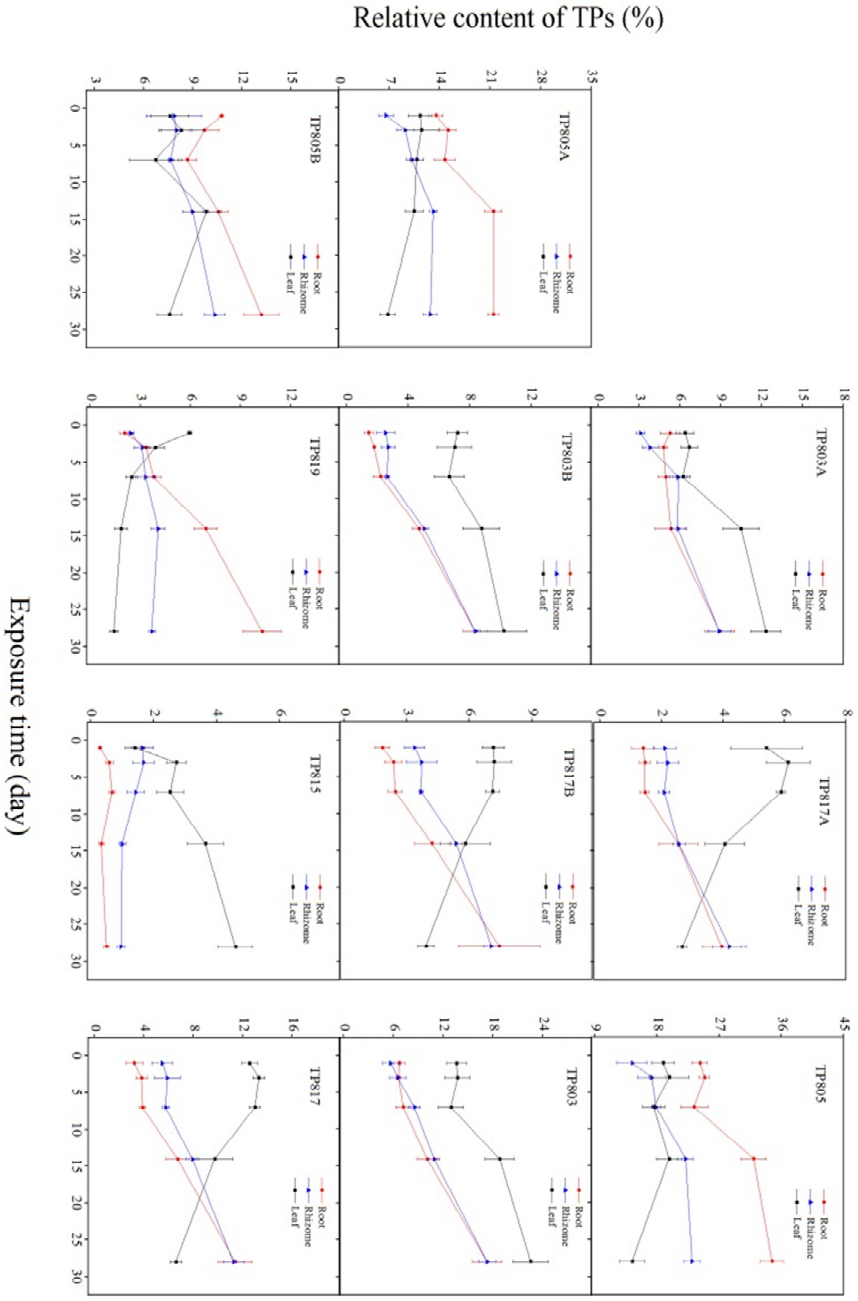
Relative content of TPs (%)
Exposure time (day)
TP805A
TP805B
TP803A
TP803B
TP817A
TP817B
TP805
TP803
TP819
TP815
TP817
Root
Rhizome
Leaf

Figure 5

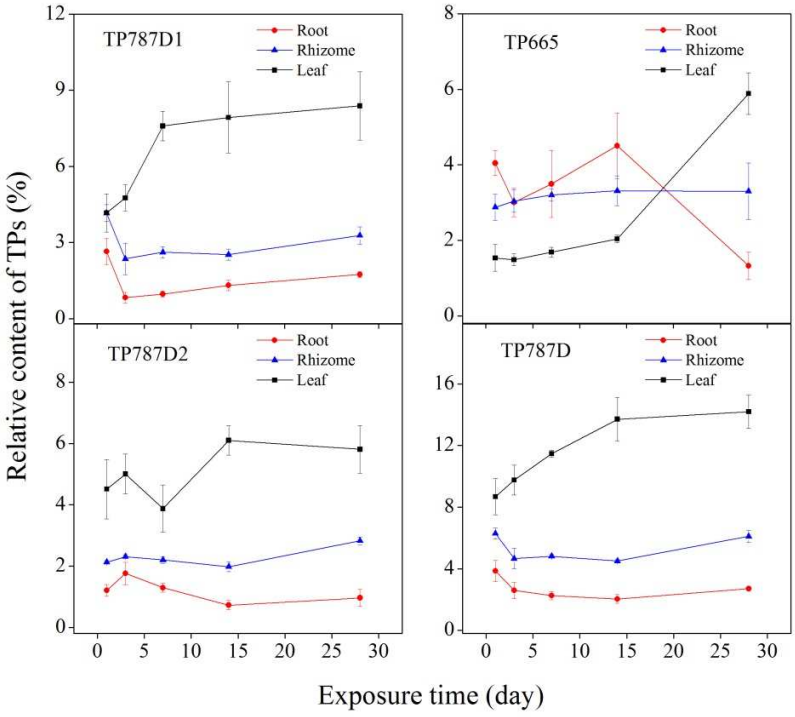

Highlights

1. The iopromide removal efficiency reached 86.6% after 28 days exposure.
2. The iopromide concentration in roots and rhizomes increased up to 7th day, thereafter decreased.
3. The iopromide concentration decreased over the whole experimental period in leaves.
4. Carboxylic transformation products were the major kind of iopromide transformation products in *T. latifolia*.
5. There are different transformation pathways of iopromide among different plant tissues.